Available online at www.sciencedirect.com

ScienceDirect

Procedia CIRP 56 (2016) 100 – 104

www.elsevier.com/locate/procedia

9th International Conference on Digital Enterprise Technology - DET 2016 – "Intelligent Manufacturing in the Knowledge Economy Era

Cutting force prediction in four-axis milling of curved surfaces with bull-nose end mill

Zhou Xu[a], Luo Ming[a,]*, Zhang Dinghua[a], Liu Wanzhu[b]

[a]*Key Laboratory of Contemporary Design and Integrated Manufacturing Technology, Ministry of Education, Northwestern Polytechnical University, Xi'an 710072, China*

[b]*AVIC Xi'an Aero-Engine (Group) Ltd, Xi'an 710021, China*

* Corresponding author. Tel.: +86 29 88493232 409. *E-mail address:* luoming@nwpu.edu.cn

Abstract

This paper presents a mechanistic model for prediction cutting forces in bull-nose end milling of curved surfaces. Firstly, a mechanistic cutting force model for bull-nose end mill is established. Secondly, the machining process characteristics for four-axis milling of ring-shaped casings are discussed. A slice-based method is proposed for prediction the cutter-workpiece engagements. Then, the cutting forces with three different lead angles are predicted and compared with the corresponding experimental values. The results show the feasibility and effectiveness of the presented prediction approach.

Peer-review under responsibility of the scientific committee of the 5th CIRP Global Web Conference Research and Innovation for Future Production

Keywords: Cutting force; Four-axis milling; Curved surfaces; Bull-nose end mill; Tool-workpiece engagements

1. Introduction

In the milling process, the cutting forces play great effects on chatter stability analysis, machining error prediction, cutting power calculation, tool wear judgment and cutting parameters optimization. Therefore, it is necessary to establish a suitable model for accurately predicting the cutting forces. Many studies have been focused on this issue.

At present, the cutting force model mainly includes the following three types: the empirical model, the analytical model and the mechanistic model, among which the third one has the most extensive influence and application. Altintas[1] developed a typical mechanistic cutting force model. In this model, cutting forces are represented as the product of cutting force coefficients and chip load. The cutting force coefficients can be identified by the approach of linear regression. Gradisek[2] presented a semi-mechanistic identification method of the coefficients for a general helical end mill from milling tests at arbitrary radial immersion. Li[3] and Gao[4] applied and improved this method in the bull-nose end milling process. The chip loads can be determined according to the engagements between the tool and the workpiece. Kim[5] calculated the cutter contact area from the Z-map of the surface geometry and current cutter location. Yang[6] proposed a solid trimming method to determine tool-workpiece engagement maps. Based on the work of Altintas, Wan[7,8] proposed an instantaneous cutting force model, in which the cutting forces are separated into two parts: a nominal component independent of the runout and a perturbation component induced by the runout.

The casings are widely used to house and protect the whole aero-engine. They are typical thin-walled parts with ring-shaped and closed geometry structures. The outer surface of a casing is a curved surface and usually machined with bull-nose end mills. The machining accuracy and the surface quality will directly affect the safety and reliability of the aero-engine. And the accurate prediction of cutting force is a key factor to achieve effective control of the machining process. However, the chip load calculation during bull-nose end milling of aero-engine casings is difficult due to the complex geometries both of the tool and the workpiece. Additionally, the multi-axis milling manner makes the

Peer-review under responsibility of the scientific committee of the 5th CIRP Global Web Conference Research and Innovation for Future Production
doi:10.1016/j.procir.2016.10.027

calculation of tool-workpiece engagement region more complicated.

In this paper, a mechanistic model for calculating cutting forces in bull-nose end milling of ring-type parts is presented. The cutting forces are predicted by considering the influences of lead angle. And several experimental tests are carried out to validate the feasibility and effectiveness of the proposed method.

2. Mechanistic cutting force model

Fig. 1 shows the envelope of a bull-nose end mill, which can be defined by four geometric parameters[1,2]: the tool diameter D, the corner radius R_c, the tool length L, and the flute length L_f. In order to clearly represent the related cutting parameters, a Cartesian tool coordinate system (TCS) is defined at the cutter tip. The z-axis is along the tool axis direction, and the x- and y-axes are on the transversal directions.

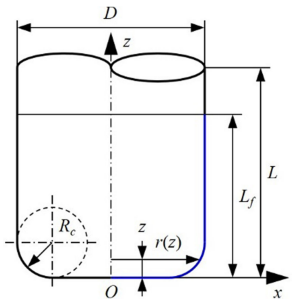

Fig. 1. Envelope of a bull-nose end mill.

The radius of the tool is variable along the z-axis, and will be calculated as:

$$r(z)=\begin{cases}\dfrac{D}{2}-R_c+\sqrt{R_c^2-(R_c-z)^2} & 0\le z\le R_c\\ \dfrac{D}{2} & R_c<z\le L_f\end{cases} \tag{1}$$

Fig. 2 shows a helical cutting edge, which is wrapped around the envelope of a bull-nose end mill. A vector ($\mathbf{r}_j$) drawn from the cutter tip (O) to any point (P) on the jth cutting edge can be expressed as:

$$\begin{aligned}\mathbf{r}_j &= x_j\mathbf{i}+y_j\mathbf{j}+z_j\mathbf{k}\\ &= r(\varphi_j)(\sin\varphi_j\mathbf{i}+\cos\varphi_j\mathbf{j})+z(\varphi_j)\mathbf{k}\end{aligned} \tag{2}$$

with

$$\varphi_j(z)=\varphi+(j-1)\varphi_p-\psi(z) \tag{3}$$

$$\varphi_p=\frac{2\pi}{N} \tag{4}$$

$$\psi(z)=\frac{2z\tan i_0}{D} \tag{5}$$

where φ_j is the radial immersion angle of point P on the jth cutting edge, φ is the rotation angle of the first cutting edge at the elevation $z = 0$, φ_p is the pitch angle of the milling cutter, $\psi(z)$ is the radial lag angle caused by the local helix angle, N is the number of flutes on the tool, i_0 is the constant helix angle of the tool.

Based on the mechanistic cutting force model presented by Altintas[1], three orthogonal cutting force components of the jth flute can be expressed as:

$$\begin{cases}dF_{t,j}(\varphi,z)=K_{tc}h_j(\varphi,\kappa)db+K_{te}ds\\ dF_{r,j}(\varphi,z)=K_{rc}h_j(\varphi,\kappa)db+K_{re}ds\\ dF_{a,j}(\varphi,z)=K_{ac}h_j(\varphi,\kappa)db+K_{ae}ds\end{cases} \tag{6}$$

with

$$h_j(\varphi,\kappa)=f_t\sin\varphi_j\sin\kappa \tag{7}$$

$$db=\frac{1}{\sin\kappa}dz \tag{8}$$

$$\begin{aligned}ds&=|d\mathbf{r}|\\ &=\sqrt{r^2(\varphi)+(r'(\varphi))^2+(z'(\varphi))^2}\,d\varphi\end{aligned} \tag{9}$$

$$\kappa(z)=\arccos\frac{R_c-z}{R_c} \tag{10}$$

where K_{tc}, K_{rc}, K_{ac} are the cutting force coefficients in tangential, radial and axial directions, respectively, K_{te}, K_{re}, K_{ae} are the edge force coefficients in tangential, radial and axial directions, respectively, $h_j(\varphi,\kappa)$ is the undeformed chip thickness, db is the projected length of the edge segment in the direction along the cutting velocity, ds is the length of the elemental edge, f_t is the feed per tooth, and $\kappa(z)$ is the axial immersion angle.

Once three force components are obtained from Eq. (6), they can be mapped into Cartesian tool coordinate system:

$$\begin{bmatrix}dF_{x,j}(\varphi,z)\\ dF_{y,j}(\varphi,z)\\ dF_{z,j}(\varphi,z)\end{bmatrix}=T_j(\varphi,\kappa)\begin{bmatrix}dF_{t,j}(\varphi,z)\\ dF_{r,j}(\varphi,z)\\ dF_{a,j}(\varphi,z)\end{bmatrix} \tag{11}$$

with

$$T_j(\varphi,\kappa)=\begin{bmatrix}-\cos\varphi_j & -\sin\varphi_j\sin\kappa & -\sin\varphi_j\cos\kappa\\ \sin\varphi_j & -\cos\varphi_j\sin\kappa & -\cos\varphi_j\cos\kappa\\ 0 & -\cos\kappa & -\sin\kappa\end{bmatrix} \tag{12}$$

The total cutting force components for the rotational position φ can be evaluated by summing the forces acting on all flutes along the axial depth of cut:

$$\begin{cases} F_x = \sum_{j=1}^{N} \int_{z_1}^{z_2} dF_{x,j}(\varphi, z) \\ F_y = \sum_{j=1}^{N} \int_{z_1}^{z_2} dF_{y,j}(\varphi, z) \\ F_z = \sum_{j=1}^{N} \int_{z_1}^{z_2} dF_{z,j}(\varphi, z) \end{cases} \quad (13)$$

where z_1 and z_2 are the contact boundaries of the flute within the cut.

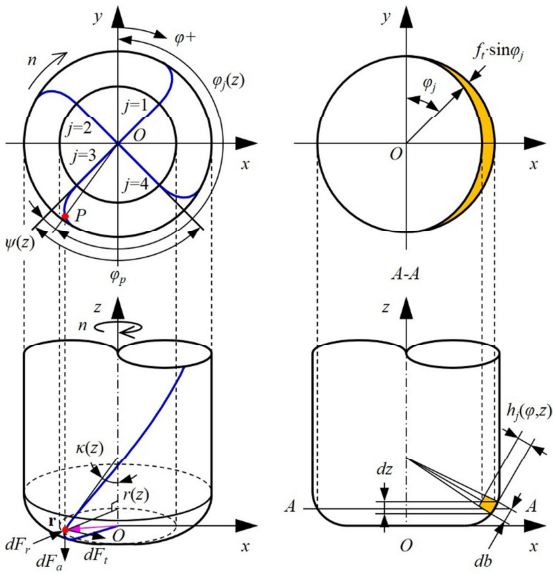

Fig. 2. Geometric model of a bull-nose end mill.

3. Calculation of tool-workpiece engagement region

In order to calculate the tool-workpiece engagement region, two other coordinate systems are defined in four-axis milling process, as shown in Fig. 3. The first one is a fixed coordinate system (MCS), formed by the *X*, *Y* and *Z* axes of the machine tool. The second one is the process coordinate system (FCN), consisting of feed *F*, cross-feed *C* and surface normal *N* axes.

In FCN, the tool-axis direction is defined by a lead angle θ, which can be determined as:

$$\theta = \arcsin \frac{d_{e1} - \left(\frac{D}{2} - R_c\right)}{R_c} \quad (14)$$

with

$$\theta = \arcsin \frac{d_{e2}}{R_m} \quad (15)$$

$$d_e = d_{e1} + d_{e2} \quad (16)$$

where R_m the machined surface radius, d_e the eccentric distance, d_{e1} the first part of the eccentric distance and d_{e2} the second part of the eccentric distance.

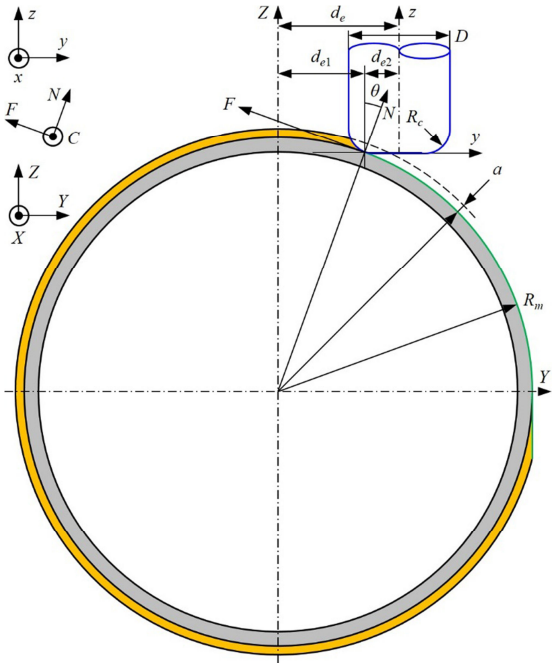

Fig. 3. Coordinate systems and lead angle.

The engagement region is located between the toroidal surface rotated by cutter edges and the workpiece solid, as shown in Fig. 4. In this paper, the previously developed method[9,10] is extended to calculate the tool-workpiece engagement region. The algorithm is as follows. Firstly, the relative position relationship between the tool and the workpiece is fixed according to the definition of lead angle. Secondly, several slices are inserted between the machined and blank surfaces to get the intersection curves between the slices and the toroidal surface. Thirdly, by determining the minimum distance from the intersection curves to the reference planes, the reference points can be obtained. Then, the engagement boundary can be fixed with a spline curve fitted by the reference points and an intersection curve between the blank surface and the toroidal surface. This method can be used in three different cutting cases: first cut, following cut and slotting cut.

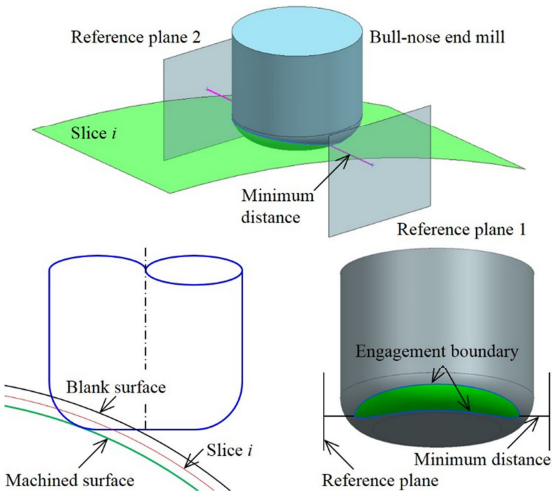

Fig. 4. Calculation of engagement region.

4. Experimental results and discussion

To validate the proposed method, several milling tests were carried out on a high-speed milling center, as shown in Fig. 5. A rotary dynamometer Kistler 9213C is used to measure the cutting forces. Cemented carbide and 304 stainless steel were used as the cutter and the workpiece materials, respectively. The tool is a bull-nose end mill with 4 flute, 12 mm diameter, 2 mm corner radius and 38° helix angle. The workpiece is a cylindrical pipe with 211mm inner diameter and 217mm outer diameter. The milling tests are a series of following cut, where the spindle speed is 5000 r/min, the feed rate is 320 mm/min, the axial depth of cut is 0.5 mm and the radial depth of cut is 6 mm.

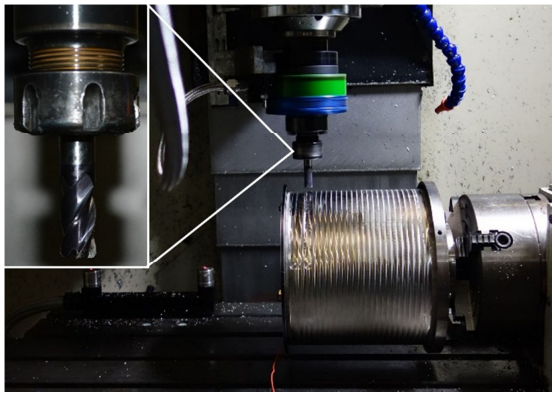

Fig. 5. Experimental setup.

The cutting force coefficients are calculated as functions of the axial depth of cut using the approach developed by Gradisek[2], as shown in Fig. 6.

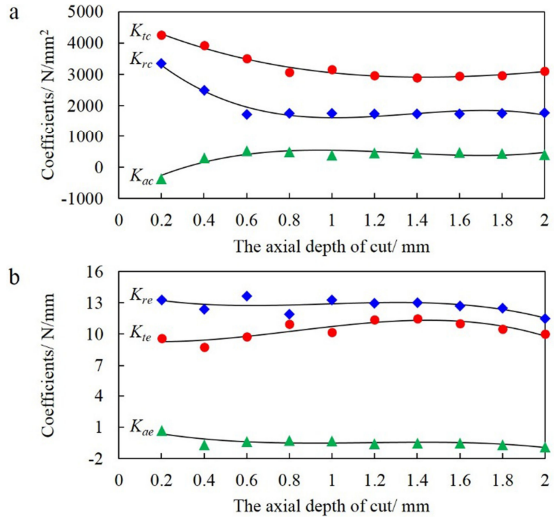

Fig. 6. (a) The cutting force coefficients; (b) the edge force coefficients.

The cutting forces with three different lead angles are determined and compared to the experimental values, as shown in Fig. 7, Fig. 8 and Fig. 9. It can be seen that the predicted and measured results have good agreements in both the magnitude and the trends. With the lead angle increasing, the cutting force F_z will decrease, and the cutting forces F_x and F_y will increase. In other words, the cutting force will decompose from the axial direction to the transverse direction with the lead angle increasing. Therefore, if the lead angle increases appropriately in the milling of aero-engine casings, the cutting force along the normal direction at the cutting position will reduce, thus, the machining deformation and vibration of the workpiece will become weak.

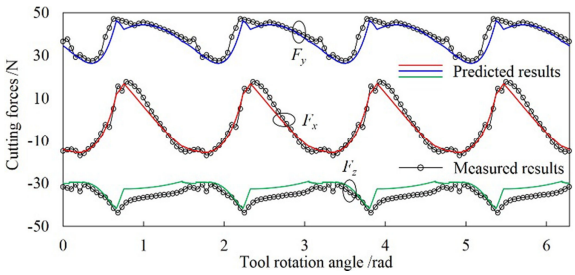

Fig. 7. Cutting forces for 0° lead angle.

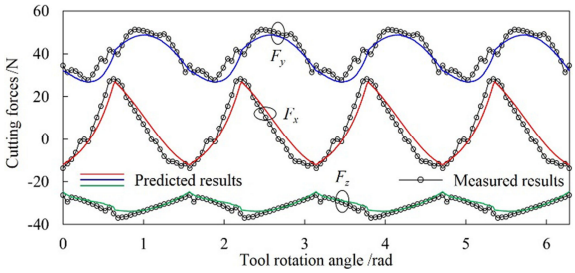

Fig. 8. Cutting forces for 4° lead angle.

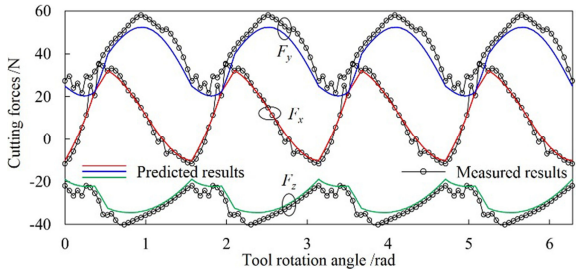

Fig. 9. Cutting forces for 8° lead angle.

As shown in Fig. 7, Fig. 8 and Fig. 9, the cutting forces F_x, F_y and F_z did not reach zero at the same time. For the case of 4° lead angle, the contact angle range φ_r is more than $\pi/2$ while the radial depth of cut equals to 6 mm, as shown in Fig. 10(a). Then, there are two tooth in cutting material. When the radial depth of cut is 1mm, the contact angle range φ_r will less than $\pi/2$, see in Fig. 10(b). Then, there is only one tooth in cutting material. The cutting forces F_x, F_y and F_z reach zero at the same time, as shown in Fig. 11.

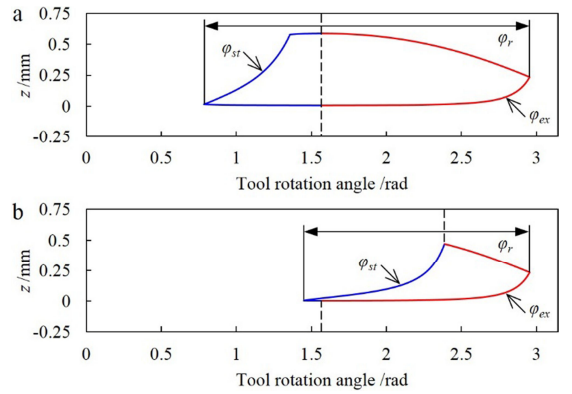

Fig. 10. Contact angles for 4° lead angle while the radial depth of cut is (a) 6mm; (b) 1mm.

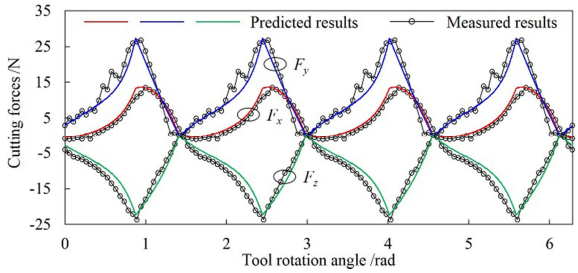

Fig. 11. Cutting forces for 4° lead angle while the radial depth of cut is 1mm.

5. Conclusions

A mechanistic cutting force model for four-axis milling of curved surfaces was presented. And the cutting forces with different lead angles were determined and compared with the corresponding experimental values. The results show the correctness and effectiveness of the presented prediction method. A slice-based method was proposed for calculating the tool-workpiece engagement regions. And the method can be used in the cutting cases with different lead angle, different axial and radial depth of cut. The effects of the lead angle on the cutting force were analyzed. With the increasing of the lead angle, the cutting force along the tool-axis direction decreases and the acting force on the tool decomposes into the transversal more. Therefore, appropriately increasing the lead angle can help control the machining deformation and vibration.

Acknowledgements

This work was supported by the National Basic Research Program of China (No. 2013CB035802) and the National Natural Science Foundation of China (No. 51305354 and No. 51475382).

References

[1] Altintas Y, Engin S. Generalized modeling of mechanics and dynamics of milling cutters. CIRP Annals - Manufacturing Technology, 2001, 50(1): 25-30.
[2] Gradisek J, Kalveram M, Weinert K. Mechanistic Identification of specific force coefficients for a general end mill. Internatinal Journal of Machine Tools and Manufacture, 2004, 44(4): 401-414.
[3] Li ZQ, Liu Q. The cutting force coefficients recognition and dynamic force modeling of the R cutter. Transactions of Chinese Society for Agricultural Machinery, 2008, 39(4): 207-211.
[4] Gao G, Wu BH, Zhang DH, et al. Mechanistic identification of cutting force coefficients in bull-nose milling process. Chinese Journal of Aeronautics, 2013, 26(3): 823-830.
[5] Kim GM, Cho PJ, Chu CN. Cutting force prediction of sculptured surface ball-end milling using Z-map. Internatinal Journal of Machine Tools and Manufacture, 2000, 40(2): 277-291.
[6] Yang Y, Zhang WH, Wan M, et al. A solid trimming method to extract cutter-workpiece engagement maps for multi-axis milling. The International Journal of Advanced Manufacturing Technology, 2013, 68(9-12): 2801-2813.
[7] Wan M, Zhang WH, Qin GH, et al. Efficient Calibration of Instantaneous Cutting Force Coefficients and runout parameters for general end mills. Internatinal Journal of Machine Tools and Manufacture, 2007, 47(11): 1767-1776.
[8] Wan M, Zhang WH, Dang JW, et al. New procedures for calibration of instantaneous cutting force coefficients and cutter runout parameters in peripheral milling. Internatinal Journal of Machine Tools and Manufacture, 2009, 49(14): 1144-1151.
[9] Wu BH, Gao G, Luo M, et al. Prediction and experimental validation of cutting force for bull-nose end mills with lead angle. Advances in Mechanical Engineering, 2014, 2014: 650215-1-15.
[10] Zhou X, Zhang DH, Luo M, et al. Chatter stability prediction in four-axis milling of aero-engine casings with bull-nose end mill. Chinese Journal of Aeronautics, 2015, 28(6): 1766-1773.